Longshore sand transport on beaches

Article *in* Journal of Geophysical Research Atmospheres · October 1970

DOI: 10.1029/JC075i030p05914

2 authors, including:

Paul D. Komar
Oregon State University
187 PUBLICATIONS **13,816** CITATIONS

SEE PROFILE

Longshore Sand Transport on Beaches

PAUL D. KOMAR AND DOUGLAS L. INMAN

Scripps Institution of Oceanography, University of California, La Jolla 92037

Simultaneous field measurements of wave and current parameters in the surf zone and the resulting longshore transport of sand have been made on two beaches under a variety of conditions. The direction and flux of wave energy was measured from an array of digital wave sensors placed in and near the surf zone. Quantitative measurements of the longshore sand transport rate were obtained from the time history of the center of gravity of sand tracer. The measurements have been used to test two models for the prediction of the longshore transport rate of sand. The first model gives the immersed weight longshore transport rate of sand, I_l, as proportional to the longshore component of wave energy flux (power), $I_l = K(ECn)_b \sin \alpha_b \cos \alpha_b$, where E is the energy density, Cn is the wave group velocity, and α_b is the breaker angle. The second model assumes that the waves provide the power to move and support the sand and that the superimposed longshore current $\langle v_l \rangle$ provides a longshore component that results in the longshore transport of sand according to the relationship $I_l = K' (ECn)_b \cos \alpha_b \langle v_l \rangle / u_m$, where u_m is the magnitude of the maximum horizontal component of orbital velocity near the bottom under the breaking wave, assumed to be proportional to the rate of energy dissipation by friction on the beach bed. The measurements show that both models successfully predict the sand transport rate, with values of the dimensionless coefficients $K = 0.77$ and $K' = 0.28$. The coherence of the models implies that they are interrelated, their common solution giving the relation as $\langle v_l \rangle = K'' u_m \sin \alpha_b$, where K'' is a dimensionless constant equal to 2.7. This relation can be obtained directly by equating the longshore current and the longshore component of the momentum flux (radiation stress) of the breaking waves. Thus, the coherence of the models appears to be based on the generation of the longshore currents by the longshore radiation stress. The models will not be equivalent if $\langle v_l \rangle$ owes its origin to some other generating mechanism such as tides or winds.

It has been recognized for many years that, when waves break at an angle to the shoreline, they cause a transport of sand along the beach. This longshore transport of sand is of great interest to the coastal engineer who is to build structures such as jetties and breakwaters that act as dams to the longshore movement of sand. It is also of interest to marine geologists in understanding the formation of spits and the transport of sand along the coasts of the world.

Grant [1943] has suggested that the longshore current combined with the agitating action of the breaking waves provides the driving force for moving sand along the beach. A report of the *Scripps Institution of Oceanography* [1947] suggests that the work performed by waves might be a useful parameter for predicting the longshore transport rate of sand by wave action. This concept has been applied by the Los Angeles District of the U.S. Army Corps of Engineers to estimate the predominant direction of sand transport from hindcast wave data [*Eaton*, 1951]. Since then, numerous laboratory and field investigations of the relation between the sand transport rate and wave and current parameters have been conducted. The field experiments of *Watts* [1953], *Caldwell* [1956], and *Ingle* [1966] all indicate that the longshore transport of sand is proportional to the longshore component of the energy flux of the waves measured at the break point. However, none of these experiments were made with sufficient resolution to permit an accurate assessment of both the sand transport rate and the energy flux of the waves.

Thus, a major limitation of our understanding of the relation between the longshore transport of sand and wave and current parameters has been the almost total lack of reliable field measurements relating the two. The development of radioactive tagging of sand grains and the more readily applied techniques of fluor-

escent tagging of sand together with the procedures of *Crickmore and Lean* [1962] made the accurate assessment of sand transport rates possible. To reliably measure the energy flux of the waves one must install wave sensor arrays in and near the surf zone and compute wave spectra and cross spectra [*Koontz and Inman*, 1967]. Field measurements using these newer tools began in 1966. In a preliminary report *Inman et al.* [1969] verified that the longshore transport rate of sand is directly proportional to the longshore component of wave power for fully developed transport conditions and showed that the factor of proportionality between the transport rate and the energy flux of the waves was larger than previously thought. Our study also shows that transport conditions in the laboratory are not fully developed and that therefore laboratory data cannot be linearly extrapolated to predict field conditions. This paper presents the results of the completed study; it is also in part a summary of the Ph.D. thesis of *Komar* [1969], which may be consulted for greater detail.

Mechanics of Transport

Two concepts or models have been proposed for the longshore transport of sand. The first is principally intuitive and attempts to correlate the sand transport rate to the longshore component of the wave energy flux per unit length of beach

$$P_l = (ECn)_b \sin \alpha_b \cos \alpha_b \qquad (1)$$

where E is the wave energy density, Cn is the wave group velocity, and α_b is the breaker angle. The subscript b denotes the wave breaker position. Energy flux has the units of power, and for that reason P_l has generally been termed 'the longshore component of wave power.' However, this term is somewhat misleading because in physics power is a scalar quantity that lacks direction.

Initial attempts to correlate sand transport to wave parameters focused on demonstrating empirical relationships between P_l and the longshore volume transport rate of sand S_l [*Watts*, 1953; *Caldwell*, 1956; *Savage*, 1959]. Such purely empirical correlations summarize the available data but have the disadvantage of being dimensionally incorrect.

Inman and Bagnold [1963] point out that the transport rate of sediment should be expressed as an immersed weight transport rate given by

$$I_l = (\rho_s - \rho) g a' S_l \qquad (2)$$

where ρ_s and ρ are respectively the sand and water densities and a' is the correction factor for pore space and can be taken as 0.6. It is advantageous to express the sand transport as an immersed weight rather than a volume because doing so takes into consideration the density of the sediment grains and permits I_l and P_l, which have the same units, to be related by

$$I_l = KP_l = K(ECn)_b \sin \alpha_b \cos \alpha_b \qquad (3)$$

where K is a dimensionless coefficient or proportionality.

This relationship was basically intuitive because no real consideration of the actual mechanics of sand transport went into its formulation. However, *Komar* [1970] shows that equation 3 can be derived directly under the assumption that the longshore transport rate of sand is equal to the longshore component of the sediment being carried forward under the bore from the breaking wave as the wave advances obliquely toward the shoreline.

Inman and Frautschy [1966] calculated the immersed weight transport rates I_l for the available field and laboratory data. A straight line with a slope of unity on a log-log plot of I_l versus P_l fitted the data then available, giving a value of K in equation 3 of 0.25.

An alternate, seemingly independent relation between the sand transport rate and the wave and current parameters was proposed by *Bagnold* [1963, p. 518] and applied to the littoral zone by *Inman and Bagnold* [1963, p. 545]. This model is based on the supposition that the orbital motion of the waves supports and moves sediment back and forth but produces no net transport even though wave energy is expended. Since the back and forth motion of the sand is supported by the wave motion, any net current superimposed on this motion will produce a net transport of sand. If some portion of the energy flux is dissipated in placing the sand in motion, the mean stress applied to the beach face is proportional to

$(ECn)_b \cos \alpha_b/u_0$, where $(ECn)_b \cos \alpha_b$ is the energy flux per unit length of beach and u_0 is the mean frictional velocity relative to the bed within the surf zone. We assume that u_0 is proportional to u_m, the maximum horizontal component of the orbital velocity near the bottom just before the wave breaks. If $\langle v_l \rangle$ is the average longshore current in the surf zone, the resulting immersed weight sand transport rate past a section of beach becomes

$$I_l = K'(ECn)_b \cos \alpha_b \langle v_l \rangle / u_m \qquad (4)$$

where K' is a dimensionless factor of proportionality. The origin of the current $\langle v_l \rangle$ is left unspecified so that the model permits a longshore transport of sand to result from a wave train arriving parallel to the shoreline ($\alpha_b = 0$) in the presence of a longshore current whose generation is not dependent on an oblique wave approach. For example, equation 4 would presumably predict the transport of sand resulting from tidal or wind-driven longshore currents in the presence of wave action.

Equations 3 and 4 provide two seemingly independent relationships for the prediction of the longshore sand transport rate from wave and current parameters. It is apparent that both models can be correct only when they are equivalent, and it will be shown that this equivalence occurs when the longshore current is due only to the longshore component of the breaking waves.

Bowen [1969a] suggested that longshore currents are generated from the longshore component of the radiation stress, where the radiation stress is defined by *Longuet-Higgins and Stewart* [1964] as the excess flow of momentum due to the presence of the waves. Following this suggestion, *Inman et al.* [1969] and *Longuet-Higgins* [1970] have independently obtained the relationship

$$\langle v_l \rangle = c_1 u_m \frac{\tan \beta}{c_f} \sin \alpha_b \cos \alpha_b \qquad (5)$$

for the longshore current, where $\tan \beta$ is the beach slope, assumed to be constant, c_f is the bottom frictional drag coefficient, u_m is the maximum horizontal component of the orbital velocity of the waves, and c_1 is a dimensionless coefficient of proportionality that *Longuet-Higgins* [1970] gives as $5\pi/8$. Substitution of this expression of $\langle v_l \rangle$ in equation 4 gives a relation that is similar to (3) but is also dependdent on the additional factor $(\tan \beta \cos \alpha_b/c_f)$. However, considerations by *Komar* [1969] suggest that

$$(\tan \beta \cos \alpha_b)/c_f = \text{constant} \qquad (6)$$

so that variation in the beach slope $\tan \beta$ does not produce a change in the longshore transport rate of sand. This possible dependence on $\tan \beta$ will be reexamined with the data obtained in this study.

Methods and Procedures

Longshore transport of sand. We obtained quantitative measurements of the longshore transport rate of sand by using sand tracers, i.e., native sand colored with a thin coating of fluorescent dye. The sand tracer was introduced onto the beach face as a single large injection of between 45 and 90 kg (100 to 200 pounds). The time history of the position of the center of gravity of the tracer as it moved along the beach was utilized to deduce the rate of advection of the sand on the beach. The movement of the sand was determined by collecting up to 200 volume samples from a grid that extended up to 450 meters along the shore and 60 meters offshore. The sample locations were closest together near the injection site and become progressively farther apart with distance from the injection line. Sampling was generally conducted between 2 and 4 hours after injection. All samples were collected with a volume sampler that penetrates the beach face to a depth of 5 cm and obtains a volume of about 450 cm^3 of sand. A sample of this size permits detection of tracer concentrations as low as one tracer grain in 10^7 to 10^8 untagged grains.

After the samples were brought back to the laboratory, washed, and dried, the number of tracer grains was counted by scanning the sample with an ultraviolet light. Tracer concentrations were expressed as the number of tracer grains per kilogram of sample. The values of tracer concentration were contoured as shown in Figure 1. Other distributions used in the study can be found in *Komar* [1969]. Following the procedure developed by *Crickmore and Lean* [1962] for rivers, we calculated the mean distance of transport from the tracer distribution by taking the first moment of the concen-

tration in the longshore direction about the injection line. Dividing this mean longshore transport distance by the elapsed time between injection and sampling then yields a mean speed for the longshore sand transport ($\langle V_l \rangle$) that is applicable to the total thickness of sand moved.

Meaningful results are obtained by this procedure only when the volume samples that the concentration diagrams are based on extend well into the beach face to the depth of burial of the sand tracer. *Ingle* [1966] used sticky cards that sampled only the top layer of sand on the beach face. Such sampling yields results that are not representative of the entire distribution of tracer and therefore are not suitable for quantitative purposes. In our study the grid sampling on the average accounted for over 80% of the total tracer introduced onto the beach.

The thickness of the layer of motion on the beach face as well as the layer's advection rate are required to compute the longshore transport rate. The thickness of the layer of motion was obtained in two ways: (1) We always assumed that the thickness of motion was equal to the depth of burial of the tracer in cores of the beach face. This requires that sufficient time for burial has elapsed, but burial appears to be quick, being complete within a half hour after tracer introduction. (2) Following *King*'s [1951] approach (which can be used only at locations where there is a sizable tidal range) we dug a series of small holes into the beach face and filled them with natural beach sand dyed with India ink. Near each we placed a stake used both to relocate the position and to determine changes in the level of the beach face. During the subsequent low tide we excavated the dyed sand sites and took the depth to which the dyed sand had been removed as a measure of the thickness of movement.

It is significant that the results of both approaches for determining the thickness of the layer of motion generally agree quite well. In spite of this, the thickness of movement is still the most uncertain of all the parameters measured. In this connection it should be recognized that the depth of burial of tracer used in this study as the thickness of the layer of motion is not an instantaneous thickness; instead it is an average that includes instantaneous motions (which may be only a few grain layers thick) as well as the effects of scour and fill produced by local adjustments in beach profile. However, because each experiment is based on a finite amount of tracer that is dispersed during a finite length of time, the depth of burial of tracer is the measure that is consistent with a transport velocity based on the new center of gravity of the tracer distribution and on the elapsed time between injection and sampling. The depth of

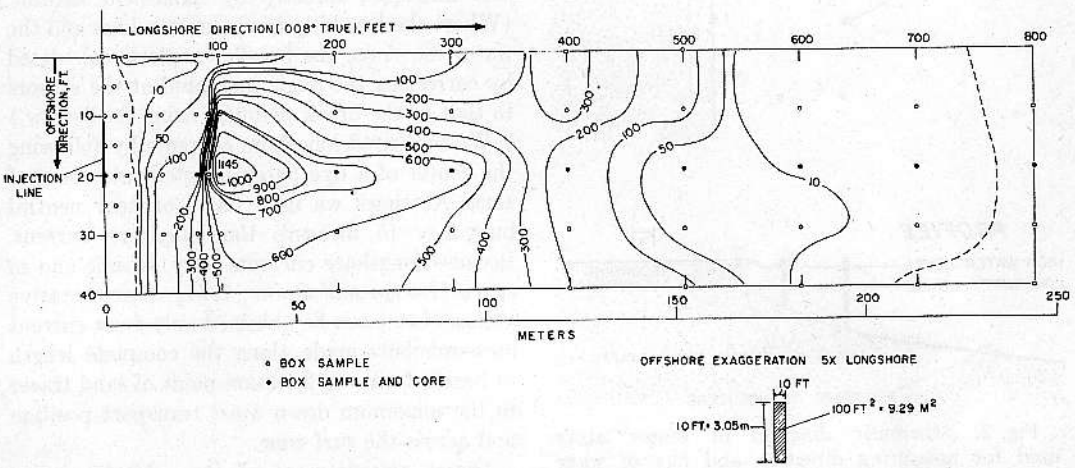

Fig. 1. Example of distribution of sand tracer along El Moreno Beach on May 5, 1966. Concentrations are in tracer grains per kilogram. Injection was 45.9 kg of El Moreno sand treated with fluorescent dye. The center of gravity of the new distribution is 75 meters from the injection line, 190 minutes after injection.

burial properly considers the total budget of tracer, and experience shows that it gives data that are coherent. This measure would lead to erroneous results if the measured thickness included layers of untagged sand, a situation which was not observed in these experiments.

If b denotes the measured thickness of movement of sand on the beach face, the bulk volume sand transport rate along the beach is given by

$$S_l = bX_b\langle V_l\rangle \tag{7}$$

where X_b is either the width of the beach face or the width of the surf zone. The immersed weight sand transport rate is then given by equation 2.

Wave and current measurements. We measured the direction and flux of wave energy from an array of digital wave sensors placed in the nearshore zone (Figure 2). The array has both onshore-offshore and longshore components with spacings between staffs of about one-quarter of the prevailing wavelength [*Koontz and Inman*, 1967].

The data output from each sensor is recorded on magnetic tape by a multi-purpose data acquisition system (DAS) and is later processed by a computer to obtain the wave spectra and cross-spectral analysis for various pairs of sensors. The wave spectrum is obtained by Fourier analysis of the time series of water level fluctuations at each sensor by using a rapid procedure modified from *Cooley and Tukey* [1965]. The individual estimates of energy density are printed out numerically and then plotted on a graph as illustrated in Figure 3. Such a graph permits the rapid identification of the wave trains arriving at the beach, a determination of their peak frequencies, and comparisons of their energies. The sum of the energy densities under the spectral peak of the incident wave train yields the mean-square elevation of the water surface $\langle\eta^2\rangle$. The wave energy per unit area of water surface is then

$$E = \rho g\langle\eta^2\rangle = \tfrac{1}{8}\rho g H_{\text{rms}}{}^2 \tag{8}$$

where H_{rms} is the root-mean-square wave height. The flux of energy per unit length of wave crest is then $P = ECn$, where the group velocity Cn is calculated from the peak period T of the wave train.

The direction of energy flux α was determined from the phase difference between pairs of sensors parallel to the shoreline and in, or just seaward of, the breakpoint of the waves. At beach locations where the wave breaker heights were low, wave breaker angles were also measured directly by hand-held sextant. (Where the breaking waves are too high and the water too deep, the breaker angle is calculated by correcting the angle measured at the sensors to that at the break point by using Snell's law.)

We measured longshore currents by following the center of a dye patch injected into the surf zone. At times we used floats of near neutral buoyancy to measure the longshore current. Because longshore currents vary in time and in space [*Inman and Quinn*, 1951], representative values of $\langle v_l\rangle$ can be obtained only from current measurements made along the complete length of beach, from the injection point of sand tracer to the maximum down coast transport position and across the surf zone.

Direct measurement of the orbital velocity near the bottom is extremely difficult and was not attempted in this study. Instead we calculated this velocity from the data obtained from

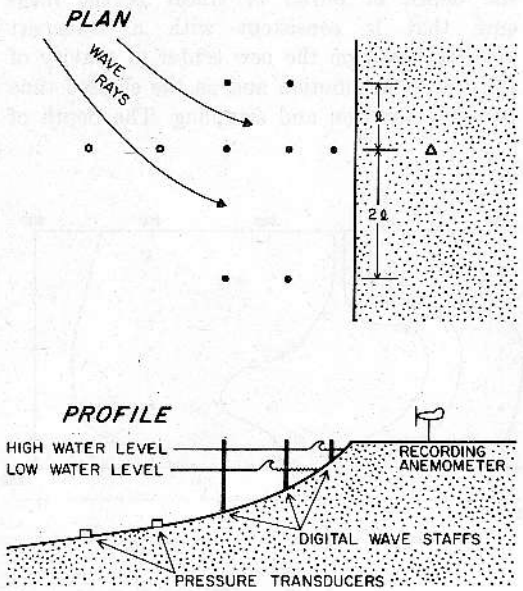

Fig. 2. Schematic diagram of sensor array used for measuring direction and flux of wave energy [after *Koontz and Inman*, 1967, Figure 16]. Spectra and cross-spectral analysis shown in Figure 3 are from a longshore pair of such an array.

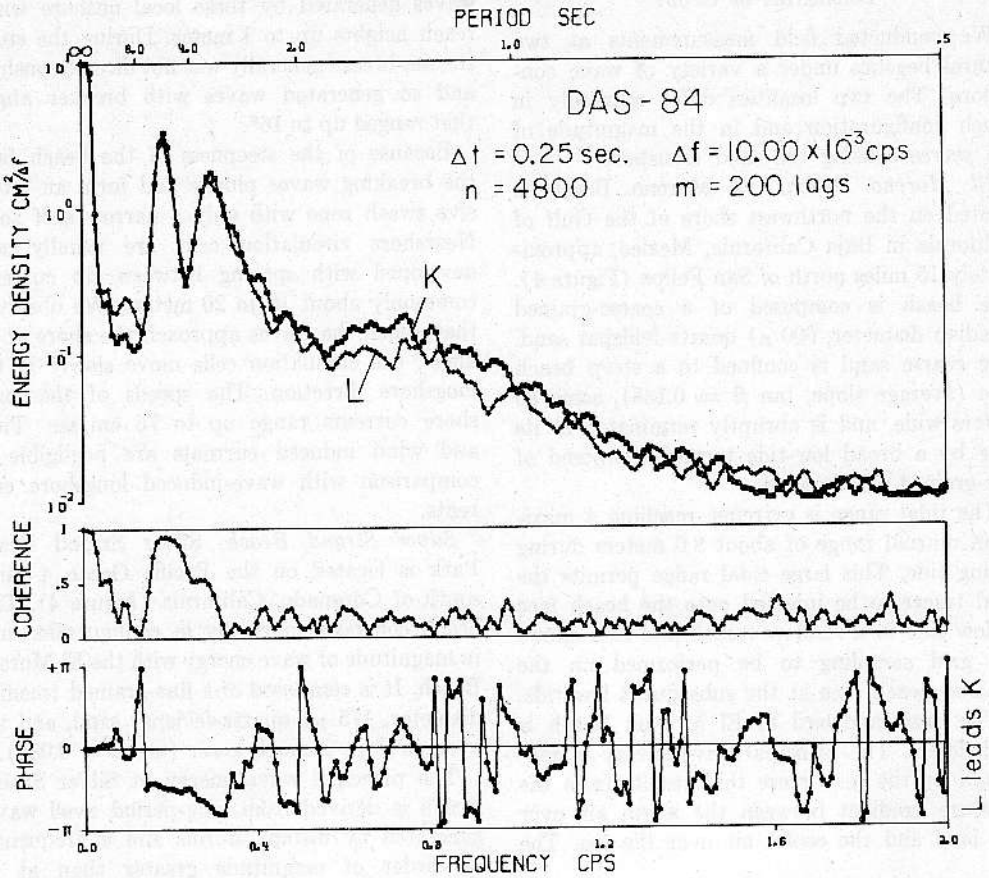

Fig. 3. Wave spectra and cross-spectral analysis for two members of an array of digital wave staffs. Staffs were parallel to the shoreline and just outside of the break point of the waves.

the energy spectrum. Whenever more than a single prominent wave train arrives at the beach, a simple calculation of a single value for u_m is not possible. On such occasions we calculated an orbital velocity that was representative of the total wave energy. Assume that H_b represents the height of the breaking wave of an imaginary wave train that combines the total energy fluxes from several superimposed wave trains according to

$$\tfrac{1}{8}\rho g H_b^2 C_b = (ECn)_{b1} + (ECn)_{b2} \qquad (9)$$

where C_b is given by linearized wave theory as

$$C_b = (gh_b)^{1/2} = (gH_b/\gamma_b)^{\frac{1}{2}} \qquad (10)$$

and $\gamma_b = H_b/h_b$ and is assumed to equal 0.78. The maximum horizontal component of the orbital velocity for this wave is

$$u_m = \tfrac{1}{2}\gamma_b C_b \qquad (11)$$

Measurements of the wave and current parameters were obtained and combined over 20-min time periods. Therefore, each 20-min data collection provides a measure of the power quantities required in the sand transport models. The quantities show some variation during any 4-hour study of sand transport. Often these variations are progressive, especially where locally generated waves are important. The sand transport results from the time average of these changing wave conditions. Therefore, the energy flux of the waves were averaged to obtain a quantitative representation of the entire period of time.

Localities of Study

We conducted field measurements at two natural beaches under a variety of wave conditions. The two localities differ markedly in beach configuration and in the magnitude of the waves causing the sand transport.

El Moreno Beach. El Moreno Beach is located on the northwest shore of the Gulf of California in Baja California, Mexico, approximately 15 miles north of San Felipe (Figure 4). The beach is composed of a coarse-grained (median diameter, 600 μ) quartz-feldspar sand. The coarse sand is confined to a steep beach face (average slope, $\tan \beta = 0.138$), some 30 meters wide, and is abruptly terminated at its base by a broad low-tide terrace composed of fine-grained muddy sand.

The tidal range is extreme, reaching a maximum diurnal range of about 8.6 meters during spring tide. This large tidal range permits the sand tracer to be injected onto the beach face at low tide in a shallow trench and also allows the grid sampling to be performed on the exposed beach face at the subsequent low tide.

The area landward of El Moreno Beach is arid desert. The principal wave energy is generated by the sea breeze that results from the pressure gradient between the warm air over the land and the cooler air over the sea. The waves generated by these local onshore winds reach heights up to 1 meter. During the study the sea breeze generally was not directly onshore and so generated waves with breaker angles that ranged up to 16°.

Fig. 4. Locations of El Moreno Beach and Silver Strand Beach, where simultaneous measurements of the longshore transport of sand and the direction and flux of wave energy were made.

Because of the steepness of the beach face, the breaking waves plunge and form an intensive swash zone with only a narrow surf zone. Nearshore circulation cells are usually well developed with spacing between rip currents commonly about 10 to 20 meters. We observed that, when the waves approach the shore at an angle, the circulation cells move slowly in the longshore direction. The speeds of the longshore currents range up to 75 cm/sec. Tidal and wind induced currents are negligible in comparison with wave-induced longshore currents.

Silver Strand Beach. Silver Strand Beach Park is located on the Pacific Ocean 4 miles south of Coronado, California (Figure 4). This beach contrasts markedly in configuration and in magnitude of wave energy with the El Moreno Beach. It is composed of a fine-grained (median diameter, 175 μ) quartz-feldspar sand, and the average slope is much lower ($\tan \beta = 0.034$).

The principal wave energy at Silver Strand Beach is derived from long-period swell waves generated by distant storms and is frequently an order of magnitude greater than at El Moreno. During the study the breaker angles were generally small, however, and reached a maximum of only 8°. Therefore, even though the total energy flux is much larger at Silver Strand than at El Moreno Beach, the longshore component of the energy flux is nearly the same. When the wave energy and angle of approach are simultaneously large, the resulting longshore component can be an order of magnitude higher than at El Moreno Beach. This difference occurred once during the study.

Because the waves break in fairly deep water, the measurements of the sand transport rates were confined to the surf and to the inner breaker zones. In calculating the immersed weight transport rate I_l we assumed that the measured sand advection rate applied throughout the entire surf zone. The tracer diagrams appear to indicate that the transport rate increases toward the breaker zone so that one might expect that the values of I_l are somewhat low [see *Komar*, 1969]. Because of this and

TABLE 1. Data Relating Longshore Sand Transport to Wave Characteristics

Date	Tide	Sand Advection Rate $\langle V_l \rangle$, cm/sec	b, cm	Volume Transport Rate S_l, cm³/sec	Immersed Weight Transport I_l, dynes/sec	Longshore Energy Flux P_l, ergs/cm sec	$(ECn)_b \cos \alpha_b \frac{\langle v_l \rangle}{u_m}$, ergs/cm sec
				El Moreno Beach			
May 4, 1966	Low	0.50	8.5	4490	45.1×10^5	43×10^5	158×10^5
May 5, 1966	Low	0.65	10.5	8380	84.4×10^5	104×10^5	254×10^5
Oct. 11, 1966	Low	0.14	10.0	2560	25.7×10^5	30×10^5	72×10^5
Oct. 13, 1966	Low	0.065	8.2	981	9.9×10^5	15×10^5	29×10^5
May 22, 1967	High	0.076	9.0	1450	14.6×10^5	20×10^5	77×10^5
May 22, 1967	Low	0.22	9.0	4260	42.8×10^5	38×10^5	116×10^5
May 23, 1967	High	0.038	7.5	604	6.1×10^5	6.0×10^5	40×10^5
May 23, 1967	Low	0.055	7.5	881	8.9×10^5	18×10^5	27×10^5
Jan. 28, 1968	Low	0.032	7.5	292	2.9×10^5	6.0×10^5	13×10^5
May 11, 1968	Low	0.14	6.0	2060	20.8×10^5	18×10^5	32×10^5
				Silver Strand Beach			
Nov. 14, 1967	High	0.099	2.0	1270	12.8×10^5	15×10^5	206×10^5
Nov. 22, 1967	High	0.55	6.0	30100	$302. \times 10^5$	380×10^5	1890×10^5
Sept. 4, 1968	High	0.15	5.0	4680	47.1×10^5	91×10^5	134×10^5
Sept. 5, 1968	High	0.12	5.5	3760	37.9×10^5	41×10^5	129×10^5

the difficulty of measuring the thickness of movement at Silver Strand Beach, the measurements of I_l at that location have a higher degree of uncertainty. Rip current spacings typically range between 100 and 500 meters and, as at El Moreno Beach, migrate slowly along shore whenever waves approach the shore at an angle. Individual longshore current measurements ranged up to 76 cm/sec.

Discussion of Results

Longshore sand transport rate. Table 1 contains the measured values of the sand advection rate $\langle V_l \rangle$ and the thickness of movement b, along with the calculated values of the volume transport rate S_l and immersed weight transport rate I_l, and also includes the corresponding time averages of the energy flux of the waves.

The corresponding measurements of the immersed weight sand transport rate I_l and the longshore component of the wave energy flux P_l are plotted in Figure 5 to test the relationship given in equation 3. It is apparent that a straight line of unit slope with a coefficient $K = 0.77$ fits the data obtained in this study very well, so that equation 3 becomes

$$I_l = 0.77 P_l \tag{12}$$

In view of the uncertainties in the sand transport measurements at Silver Strand Beach, the data agree surprisingly well with the best-fit straight line. Additional measurements probably would reveal more variation than shown.

The good agreement between the data from the two locations, whose beach slopes differ by a factor of 4, indicates that the coefficient K in the relationship between I_l and P_l is independent of the beach slope. The results also indicate that the relationship is independent of the sand size within the range of about 175 to 600 μ included in the study. In suspended load transport the size of the sediment grains is an important variable because of the dependence of the settling velocity on size. The results therefore suggest that the suspended load transport of sand in the surf zone is less important than bed load transport.

The field and laboratory results from the previous studies are also included in Figure 5. It is apparent that the measurements of the longshore energy flux obtained in this study are about one-half the value from previous field studies for a given transport rate. This discrepancy appears to result from the erroneous use of the significant wave height in computing wave energy for the earlier field observations as suggested by *Inman and Frautschy* [1966]. *Longuet-Higgins* [1952], by assuming that a wave spectrum consists of a narrow band of fre-

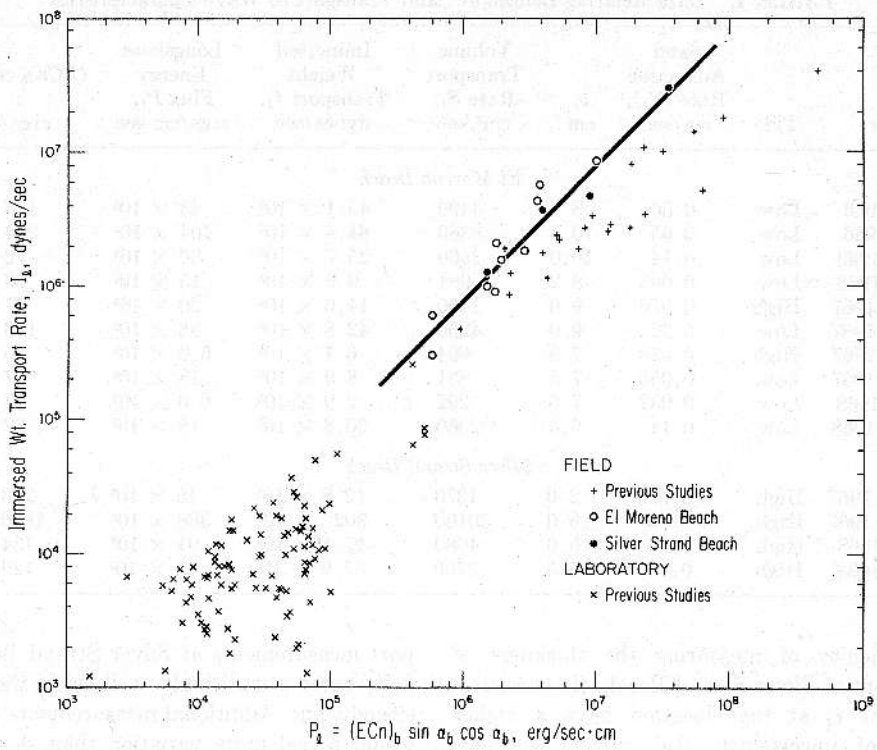

Fig. 5. Relationship between the immersed weight longshore sand transport rate and the longshore component of wave energy flux per unit length of beach. The new data are listed in Table 1 and the various sources for the 'previous studies' are given in *Inman et al.* [1969].

quencies and that the wave energy comes from a large number of different sources whose phase is random, deduced that the ratio of the significant wave height to the rms wave height $H_{1/3}/H_{rms}$ should have a value of 1.418. If this is true, the wave energy calculated from the significant wave height would be a factor of 2 higher than the energy correctly calculated from H_{rms}. This would then account for the difference between the energy flux calculations of this study and those of the previous studies.

To examine this, sets of wave data have been analyzed both by the significant wave height approach and by spectra analysis. The data acquisition system provides a 20-min analog record as well as a digital record of the waves; hence such a comparison can readily be made. The results of several such comparisons [*Komar*, 1969] indicate that the analysis of *Longuet-Higgins* [1952] generally applies to the field data of this study and thus explains the discrepancy between the results of this and previous field studies.

Figure 5 also shows that the laboratory measurements fall well below the extension of the straight line established by the field data. We believe that the reason for this is the lack of fully developed transport conditions in these laboratory studies. In the transport of sand by rivers the immersed weight sand transport rate is proportional to the available power with a constant proportionality factor only when fully developed flow is achieved [*Bagnold*, 1966]. Under lower flow regimes that are not fully developed the efficiency of utilization of the available power to transport sand is less and the proportionality factor is lower and is no longer constant. A similar effect can be expected to occur in the transport of sand on beaches so that the transport mechanism is less efficient for the laboratory studies than it is in the field. This difference in efficiency must

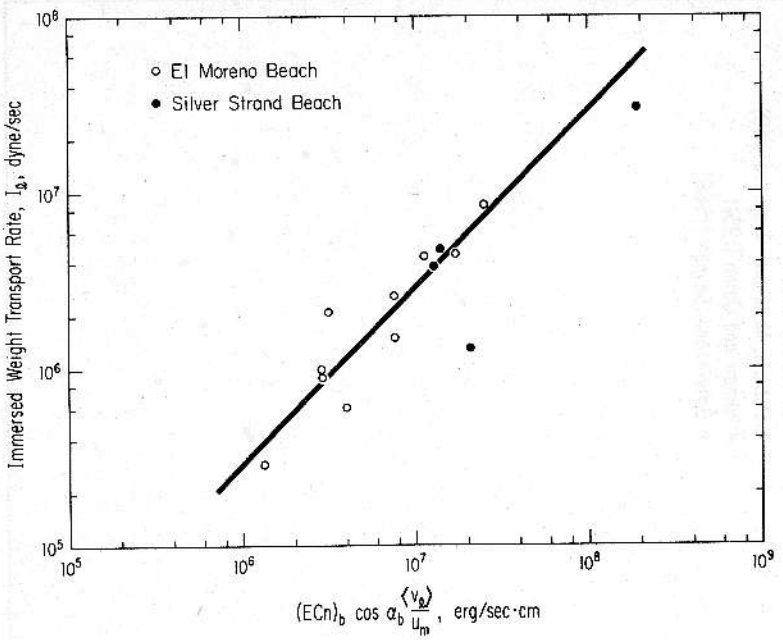

Fig. 6. Relationship between the immersed weight longshore sand transport rate and the energy flux terms of equation 4. Plotted data are listed in Table 1.

be considered in any attempts to extrapolate laboratory measurements to field conditions.

The straight line of Figure 5 and therefore equation 12 represent fully developed transport conditions and predict the maximum transport possible for a given wave situation. Plotted positions of less efficient transport conditions can be expected to fall below this line, which forms an upper limit. This is seen to be the situation for the laboratory data included in Figure 5.

The corresponding measurements of the sand transport rate I_l and the quantity $(ECn)_b \cos \alpha_b \langle v_l \rangle / u_m$ of equation 4, listed in Table 1, are plotted in Figure 6. Although the scatter of the data is somewhat greater than for the previous model, it is apparent that the data follow a trend that yields the relationship

$$I_l = 0.28(ECn)_b \cos \alpha_b \frac{\langle v \rangle_l}{u_m} \qquad (13)$$

as the best fit. Therefore, even though the two models are conceptually different, the data

TABLE 2. Longshore Currents

DAS	$\langle v_l \rangle$, cm/sec	u_m, cm/sec	α_b, deg	$u_m \tan \beta \sin \alpha_b \cos \alpha_b$, cm/sec	$u_m \sin \alpha_b$, cm/sec
55	50.0	77.7	10	1.84	13.4
59	61.0	85.6	13.5	2.68	20.0
60	54.0	88.7	14.5	2.96	22.2
61	46.4	88.3	13	2.67	19.9
62	49.4	86.8	14	2.82	21.0
63	47.0	86.3	15	2.98	22.4
73	45.7	68.9	16	2.52	19.0
76	40.0	63.8	16	2.33	17.6
79	14.1	64.4	8.8	1.34	9.8
84	15.2	66.8	8	1.27	9.2
92	27.8	68.4	7	1.14	8.3
94	48.8	77.7	11.5	2.10	15.5
95	36.0	81.5	13	2.46	18.3
96	48.8	81.9	11	2.12	15.6
97	30.5	85.7	11	2.22	16.4
1	7.6	67.7	3	0.49	3.5
3	6.9	65.5	3	0.47	3.4
173	8.1	73.0	2.8	0.48	3.6
174	15.2	74.8	2.8	0.49	3.7
175	20.1	72.7	7	1.21	8.9
176	22.3	76.1	7	1.27	9.3
198*	14.6	96.7	6	0.30	10.1

*Values for Silver Strand Beach. All other values are for El Moreno Beach.

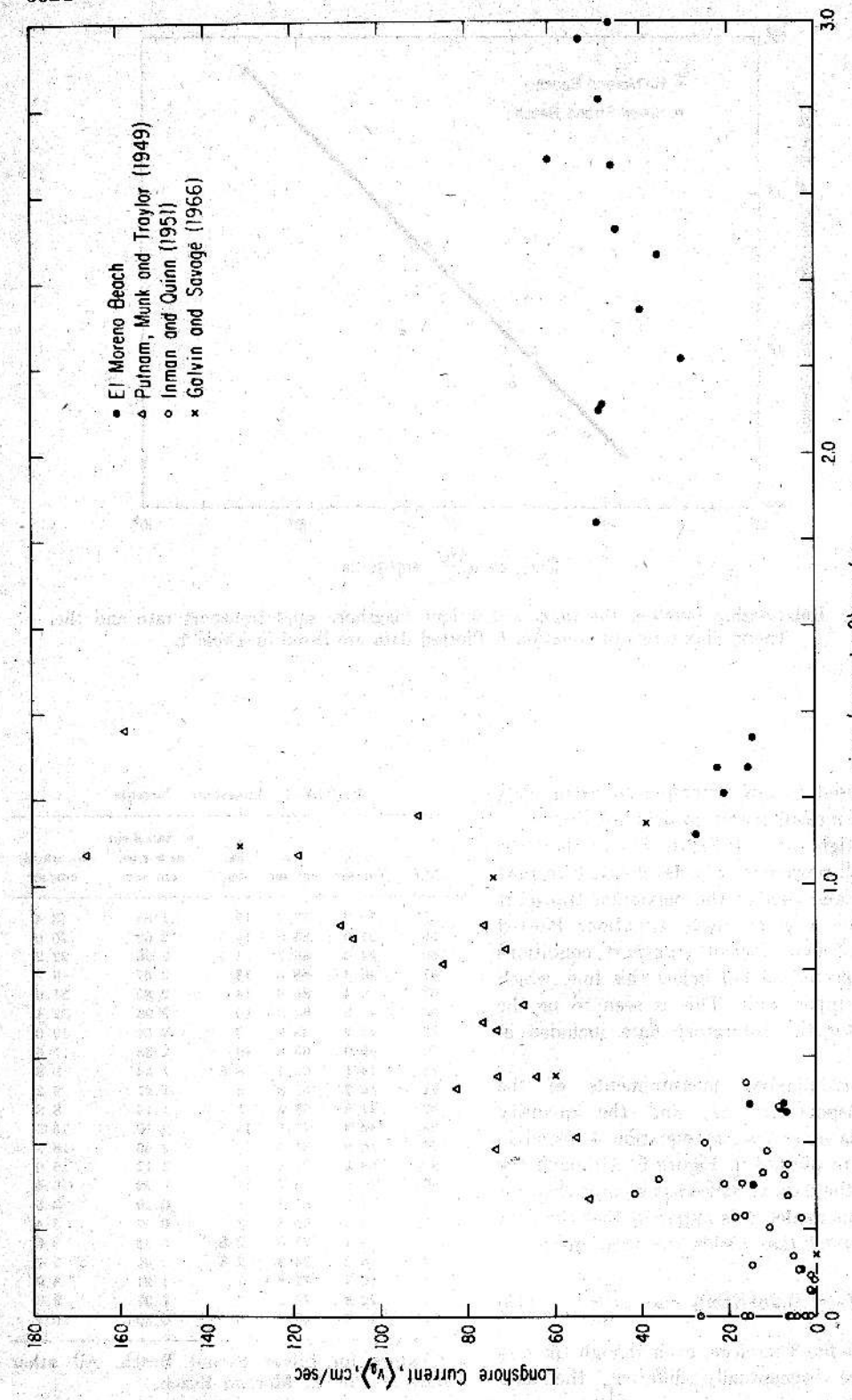

Fig. 7. Relationship between the average longshore current and the quantity determined from a consideration of the longshore component of radiation stress (equation 5). The data plotted for El Moreno Beach are listed in Table 2 (compare with Figure 8).

obtained in this study confirm both. It appears that, when the longshore current and the longshore sand transport are due to an oblique wave approach, the two models are equivalent. A simple simultaneous solution of equations 3 and 4 yields the relationship

$$\langle v_l \rangle = (K/K')u_m \sin \alpha_b \qquad (14)$$

This result is similar to equation 5 for the generation of the longshore current by the radiation stress, except for the presence of the factor tan β cos α_b/c_f. *Komar* [1969] indicates that the factor tan β cos α_b/c_f appears to be nearly constant.

To examine this point further, the parameters u_m (tan β cos α_b)sin α_b and u_m sin α_b have been computed for the runs in which only a single wave train predominated. The results are given in Table 2 along with the measured values of $\langle v_l \rangle$ and are plotted in Figures 7 and 8. Also included in the plots are the field measurements of *Putnam et al.* [1949], *Inman and Quinn* [1951], and *Galvin and Savage* [1966] as tabulated in *Galvin and Nelson* [1967]. Compari-

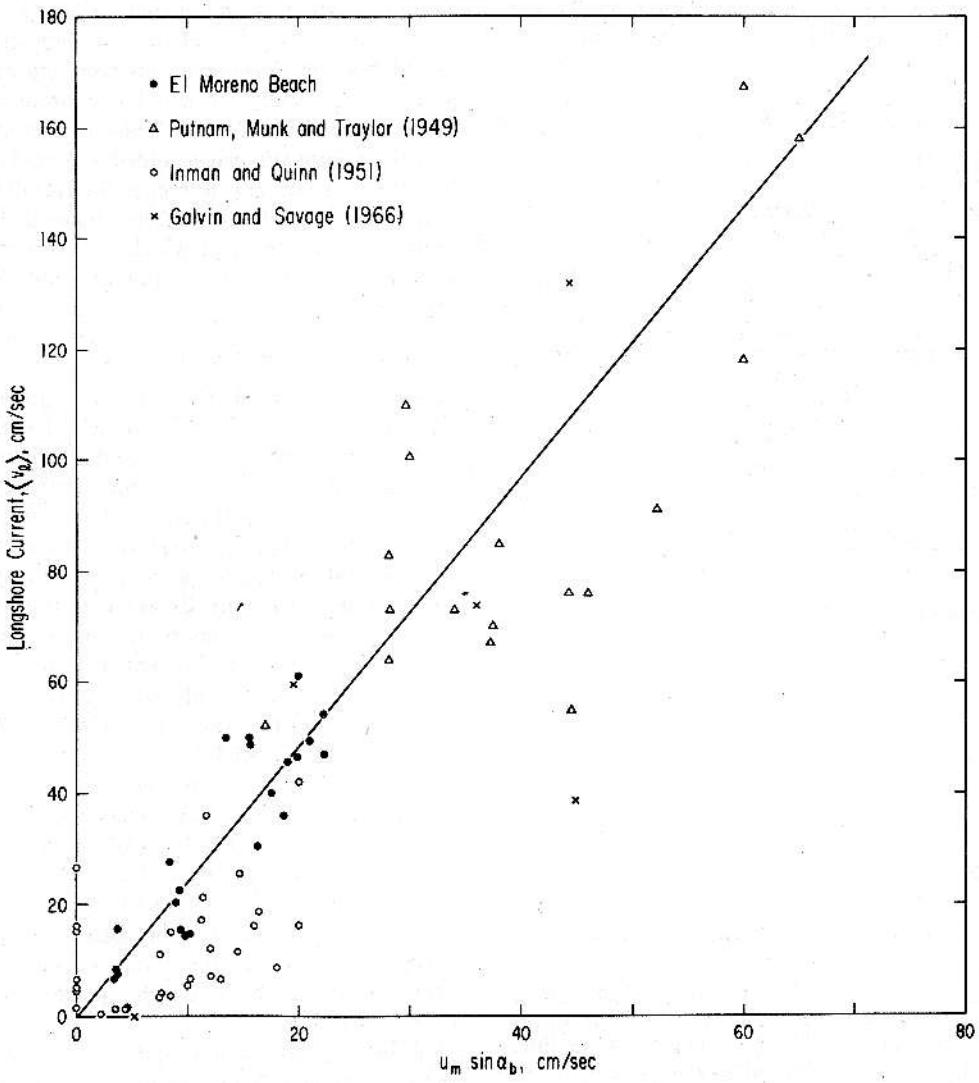

Fig. 8. A replot of the data shown in Figure 7, under the assumption that the ratio tan β cos α_b/c_f in equation 5 is constant as indicated by *Komar* [1969].

son of the two figures confirms the validity of equation 14 and indicates that the ratio $\tan \beta \cos \alpha_b / c_f$ is nearly constant. This explains the apparent lack of dependence on beach slope of both proportionality coefficients K and K'.

The relationship between the sand transport and the nearshore circulation of water requires further comment. *Bowen* [1967, 1969*b*] and *Bowen and Inman* [1969] have shown that interactions between an incoming wave train and edge waves generated in the nearshore region control the spacing between rip currents and result in circulation cells like those shown in Figure 9*A*. Under an oblique wave attack the circulation cells have been observed to move slowly along the shore; the motion is made apparent by the migration of the rip currents. Because of this migration there will be no net longshore transport of sand resulting from the symmetrical diverging currrents in the cell. At any one position on the beach the transport will be first in one direction and then in the opposite direction as the cells migrate and the cell current over the position reverses. In our measurements of the average longshore current over the entire cell $\langle v_l \rangle$ the currents of the circulation cell of Figure 9*A* average out owing to the symmetry. The residual average in the longshore current is the current generated by the longshore component of the radiation stress. It will be nearly constant in direction and magnitude so that its effect will be to produce a net longshore drift of sand. This current illustrated in Figure 9*B*, when added vectorally to the circulation system of Figure 9*A*, results in the nearshore circulation pattern shown in Figure 9*C*. It is this system which is observed in the field whenever waves approach obliquely to the shoreline.

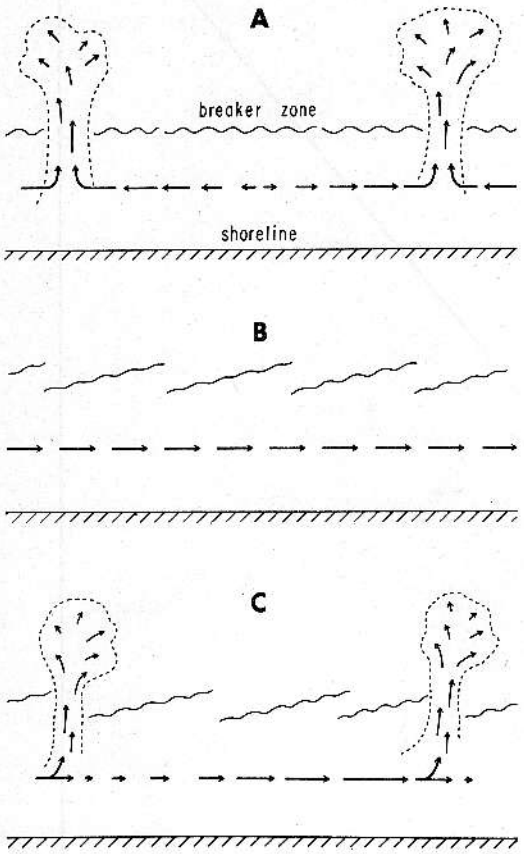

Fig. 9. (*A*) The nearshore circulation resulting from the interaction of the incident waves with edge waves. (*B*) The longshore water drift due to the longshore component of the wave momentum flux. (*C*) The vector sum of the currents shown in parts *A* and *B* to give the observed currents.

Summary

The data collected by this and previous studies clearly show that the immersed weight longshore transport rate of sand is directly proportional to the longshore component of the wave energy flux arriving at the beach as predicted by the first model (equations 3 and 12).

The second model, proposed by *Inman and Bagnold* [1963] whereby the wave motion provides the stress to support the sand and a superimposed longshore current causes a net transport, also successfully relates the sand transport rate to the wave and current parameters (equations 4 and 13).

From the equivalence of the two models it is deduced that the average longshore current resulting from the oblique approach of waves is proportional to $u_m \sin \alpha_b$. This differs from the relationship obtained from the generation of the longshore current by the longshore component of the radiation stress by only the factor $\tan \beta \cos \alpha_b / c_f$, which appears to be nearly constant.

The two models are not equivalent if a component of the longshore current is generated by some other mechanism such as tides or winds. In this situation the second model (equation 4)

appears to be more flexible and would presumably predict the longshore transport of sand, providing that the longshore current is known.

Acknowledgments. We are indebted to Professors R. S. Arthur and M. S. Longuet-Higgins, whose advice has been most helpful in conducting this study, and to C. E. Nordstrom, W. A. Koontz, E. A. Murray, S. W. Roberts, and R. J. Mann, who aided in the collection, collocation, and analysis of the field data.

This study was supported by the Coastal Engineering Research Center, U.S. Army Corps of Engineers, and by the Office of Naval Research under contract with the University of California. Komar was supported for two years by a National Science Foundation Fellowship.

References

Bagnold, R. A., Mechanics of marine sedimentation, in *The Sea*, vol. 3, pp. 507–528, edited by M. N. Hill, Interscience, New York, 1963.

Bagnold, R. A., An approach to the sediment transport problem from general physics, *U.S. Geol. Surv. Prof. Pap. 422-1*, 37 pp., 1966.

Bowen, A. J., Rip currents, Ph.D. thesis, University of California, San Diego, 1967.

Bowen, A. J., The generation of longshore currents on a plane beach, *J. Mar. Res., 37*, 206–215, 1969*a*.

Bowen, A. J., Rip currents, 1, Theoretical investigations, *J. Geophys. Res., 74*, 5467–5478, 1969*b*.

Bowen, A. J., and D. L. Inman, Rip currents, 2, Laboratory and field observations, *J. Geophys. Res., 74*, 5479–5490, 1969.

Caldwell, J. M., Wave action and sand movement near Aneheim Bay, California, Beach Erosion Board, *U.S. Army Corps Eng. Tech. Memo. 68*, 21 pp., 1956.

Cooley, J. W., and J. W. Tukey, An algorithm for the machine calculation of complex Fourier series, *Math. Comput., 19*, 297–301, 1965.

Crickmore, M. J., and G. H. Lean, The measurement of sand transport by means of radioactive tracers, *Proc. Royal Soc. London, A, 266*, 402–421, 1962.

Eaton, R. O., Littoral processes on sandy coasts, *Proc. First Conf. Coastal Eng.*, pp. 140–154, Council on Wave Research, University of California, 1951.

Galvin, C. J., Jr., and R. A. Nelson, Compilation of longshore current data, *U.S. Army Coastal Eng. Res. Center Misc. Pap. 2-67*, 19 pp., 1967.

Galvin, C. J., Jr., and R. P. Savage, Longshore currents at Nags Head, North Carolina, *U.S. Army Coastal Eng. Res. Center Bull., 11*, 11–29, 1966.

Grant, U. S., Waves as a sand transporting agent, *Amer. J. Sci., 241*, 117–123, 1943.

Ingle, J. C., Jr., The movement of beach sand, in *Developments in Sedimentology*, vol. 5, 221 pp., Elsevier, New York, 1966.

Inman, D. L., and R. A. Bagnold, Littoral processes, in *The Sea*, vol. 3, pp. 529–533, edited by M. N. Hill, Interscience, New York, 1963.

Inman, D. L., and J. D. Frautschy, Littoral processes and the development of shorelines, *Coastal Engineering*, pp. 511–536, American Society Civil Engineers, New York, 1966.

Inman, D. L., P. D. Komar, and A. J. Bowen, Longshore transport of sand, *Proc. Eleventh Conf. Coastal Eng., vol. 1*, pp. 298–306, American Society of Civil Engineers, New York, 1969.

Inman, D. L., and W. H. Quinn, Currents in the surf zone, *Proc. Second Conf. Coastal Eng.*, pp. 24–36, Council on Wave Research, University of California, 1951.

Inman, D. L., R. J. Tait, P. D. Komar, and C. E. Nordstrom, Dispersion of water and sediment in the surf zone, *Scripps Inst. Oceanogr. SIO Ref. 69-10*, University of California, San Diego, 1969.

King, C. A. M., Depth of disturbance of sand on sea beaches by waves, *J. Sediment. Petrol., 21*, 131–140, 1951.

Komar, P. D., The longshore transport of sand on beaches, Ph.D. thesis, University of California, San Diego, 1969.

Komar, P. D., The mechanics of sand transport on beaches, *J. Geophys. Res., 75*, in press, 1970.

Koontz, W. A., and D. L. Inman, A multipurpose data acquisition system for instrumentation of the nearshore environment, *U.S. Army Coastal Eng. Res. Center Tech. Memo. 21*, 38 pp., 1967.

Longuet-Higgins, M. S., On the statistical distribution of the height of sea waves, *J. Mar. Res., 11*, 245–266, 1952.

Longuet-Higgins, M. S., Longshore currents generated by obliquely incident sea waves, 1 and 2, *J. Geophys. Res., 75*(33), 1970.

Longuet-Higgins, M. S., and R. W. Stewart, Radiation stresses in water waves; a physical discussion with applications, *Deep-Sea Res., 11* 529–562, 1964.

Putnam, J. A., W. H. Munk, and M. A. Traylor, The prediction of longshore currents, *Trans. AGU, 30*, 337–345, 1969.

Savage, R. P., Laboratory study of the effect of groins on the rate of littoral transport, Beach Erosion Board, *U.S. Army Corps Eng. Tech. Memo. 114*, 55 pp., 1959.

Scripps Institution of Oceanography, A statistical study of wave conditions at five locations along the California coast, *Univ. Calif. Wave Rep. 68*, 34 pp., San Diego, 1947.

Watts, G. M., Study of sand movement at South Lake Worth Inlet, Florida, *Beach Erosion Board, U.S. Army Corps Eng. Tech. Memo. 42*, 24 pp., 1953.

(Received December 19, 1969;
revised July 7, 1970.)